

# Postpolymerization Grafting of Aniline Tetramer on Polythiophene Chain: Structural Organization of the Product and Its Electrochemical and Spectroelectrochemical Properties

Katarzyna Buga,<sup>†</sup> Agnieszka Majkowska,<sup>†</sup> Rafal Pokrop,<sup>†</sup> Malgorzata Zagorska,<sup>\*,†</sup>  
David Djurado,<sup>‡</sup> Adam Pron,<sup>‡</sup> Jean-Louis Oddou,<sup>§</sup> and Serge Lefrant<sup>||</sup>

Faculty of Chemistry, Warsaw University of Technology, Noakowskiego 3, 00-664 Warsaw, Poland,  
DRFMC, UMR 5819-SPrAM (CEA-CNRS–Université J. Fourier-Grenoble I), 38054 Grenoble Cedex 9,  
France, DRDC, UMR 5155-PMB (CEA-CNRS–Université J. Fourier-Grenoble I),  
38054 Grenoble Cedex 9, France, and Institut des Matériaux Jean Rouxel, 2 rue de la Houssinière,  
B.P.32229, 44322 Nantes Cedex 3, France

Received April 14, 2005. Revised Manuscript Received August 25, 2005

We describe the preparation of solution-processible hybrid polymers, consisting of a polythiophene main chain and randomly distributed alkyl and oligoaniline side groups. The proposed procedure involves three steps: copolymerization of alkyl- and ester-group-substituted thiophenes to give the precursor polymer, followed by the hydrolysis of the pendant ester groups and aniline tetramer grafting through an amidation reaction. The proposed method is more versatile than previously used copolymerization procedures because higher tetraaniline grafting levels can be obtained. The postfunctionalized polymer is electrochemically active both in its oligoaniline part and in its conjugated polythiophene main chain. As shown by complementary voltammetric and UV–vis–NIR and Raman spectroelectrochemical studies, the polymer can be electrochemically doped selectively in its side oligoaniline chains or globally in the main chain as well as in the side chains. Selective side-chain doping can also be achieved chemically through protonation of the grafted oligoaniline groups in their semi-oxidized state. Doping with FeCl<sub>3</sub> is global and involves the oxidation of the main chain and Lewis acid complexation of the side chains, as shown by Mössbauer spectroscopy.

## Introduction

Polythiophenes and polyanilines are the two most extensively studied families of electroactive polymers.<sup>1,2</sup> The main reason for this interest is their processibility combined with their better stability as compared to other polyconjugated systems. As a result, in many attempts at technological applications of conjugated polymers, polyaniline or polythiophene derivatives have been used in their undoped state as organic semiconductors or in the doped state as organic metals. Spectacular examples of this research direction are the fabrication of poly(alkylthiophene)-based field-effect transistors (FETs),<sup>3–6</sup> the use of undoped polyaniline as a charge dissipation component in high-voltage cables,<sup>7–9</sup> and the application of doped poly(ethylenedioxythiophene)

(PEDOT) or doped polyaniline (PANI) in electrolytic capacitors,<sup>10,11</sup> to name a few.

Although polythiophene derivatives and polyaniline are sometimes used in similar applications, their redox and acid–base chemistries are significantly different. Moreover, they are rendered processible using different processibility inducing methods.<sup>12</sup> Polythiophene derivatives exhibit principally redox-type chemistry and the switching between the undoped (semiconducting) and the doped (conducting) states is achieved by electrochemical or chemical oxidation (p-doping) or reduction (n-doping). Polyaniline can also be doped in a redox type reaction (oxidation); however, this oxidation can lead either to the doped state of the polymer or to its semi-oxidized neutral (undoped) state if the redox reaction is accompanied by an acid–base act of deprotonation. In other words, in the case of polyaniline, switching between the semiconducting state and the conducting state can be achieved not only in the redox process but also in the acid–base reaction of protonation.<sup>12</sup> Because of the importance of the acid–base chemistry (in the Brönsted sense), the electrochemical activity of polyaniline in aprotic electrolytes is distinctly different from that observed in electrolytes

\* To whom correspondence should be addressed. E-mail: zagorska@ch.pw.edu.pl.

<sup>†</sup> Warsaw University of Technology.

<sup>‡</sup> DRFMC, UMR 5819-SPrAM.

<sup>§</sup> DRFMC/SCIB/CC CEA, UMR 5155-PMB, Grenoble.

<sup>||</sup> Institut des Matériaux Jean Rouxel.

- (1) Nalwa, H. S., Ed. *Handbook of Organic Conductive Molecules and Polymers*; John Wiley & Sons: Chichester, U.K., 1997.
- (2) Skotheim, T. A.; Elsenbaumer, R. L.; Reynolds, J. R., Eds. *Handbook of Conducting Polymers*; Marcel Dekker: New York, 1998.
- (3) Ficker, J.; Ullmann, A.; Fix, W.; Rost, H.; Clemens, W. *J. Appl. Phys.* **2003**, *94*, 2638.
- (4) Stutzmann, N.; Friend, R. H.; Sirringhaus, H. *Science* **2003**, *299*, 1881.
- (5) Backlund, T. G.; Sandberg, H. G. O.; Osterbacka, R.; Stubb, H.; Makela, T.; Jussila, S. *Synth. Met.* **2005**, *148*, 87.
- (6) Bao, Z. *Adv. Mater.* **2000**, *12*, 227.
- (7) Cottevieuille, D.; Le Méhauté, A.; Challioui, C. *J. Chim. Phys.* **1999**, *5*, 1502.

(8) Kieffel, Y.; Travers, J. P.; Cottevieuille, D.; *Annu. Rep. Conf. Electron. Insul. Dielectr. Phenom.* **2000**, *1*, 52.

(9) Kieffel, Y.; Travers, J. P.; Planes, J. *Synth. Met.* **2003**, *135*, 325.

(10) Kudoh, Y.; Akami, K.; Matsuya, Y. *Synth. Met.* **1999**, *102*, 973.

(11) Uehara, H.; Yoshikawa, T.; Hu, Y.; Sasaki, S.; Yano, Y.; Doudou, T. U.S. Patent 6,042,740, 1998.

(12) Pron, A.; Rannou, P. *Prog. Polym. Sci.* **2002**, *27*, 135.

containing an efficient source of protons.<sup>13</sup> To the contrary, in the case of polythiophene derivatives, the acid–base processes accompanying the redox doping are of negligible importance.

Another important difference between the polythiophene and polyaniline families must be pointed out. Solution processibility of polythiophenes is usually achieved by branching flexible  $sp^3$ -hybridized side groups onto the conjugated main chain. This procedure does not influence, to a significant extent, the electrochemical activity of the polymer and its conductivity after doping. Moreover, by the selection of the flexible substituent, it is possible to tune the width and the position of the band gap by changing the electron-donating (-accepting) properties of the group located next to the conjugated main chain. Lowering of the oxidation potential value in polythiophenes by replacing alkyl substituents with alkoxy ones is a spectacular example of this effect.<sup>14</sup> The solubilizing methods typically used for polythiophene cannot be applied to polyaniline because either ring- or N-substitution with alkyl or alkoxy groups always leads to a significant worsening of the electrochemical properties of the polymer and its conductivity after doping. Another approach is therefore used in this case. Leaving the polymer main chain chemically unchanged in terms of covalent chemistry, it is possible to render polyaniline processible by introducing solubilizing or plasticizing groups as an inherent part of the doping (protonating) agent.<sup>15</sup>

It therefore seems interesting to develop a new class of “hybrid” polymers that would combine the redox, acid–base, and processing properties of polythiophenes and polyanilines. This can be done, for example, by branching oligoaniline side groups to the conjugated polythiophene main chain. Few attempts at grafting oligoanilines onto conventional polymers<sup>16</sup> and conjugated polymers<sup>17</sup> have been reported. In the latter case, a poly(alkylthiophene)-containing oligoaniline side chain has been prepared by copolymerization of 3-octylthiophene and thiophene functionalized with aniline tetramer. This method is of limited use, however, because of the distinctly different reactivities of both comonomers. In our previous paper,<sup>18</sup> we described a simple method of poly(alkylthiophene) postpolymerization functionalization with aromatic amines. It therefore seemed interesting to us to exploit this method for the preparation of new “hybrid” poly(alkylthiophene)-based polymers containing pendant aniline tetramer groups. We have selected aniline tetramer because this is the shortest aniline oligomer that mimics the behavior of polyaniline. The presented polymers can be considered as random copolymers of alkylthiophenes and thiophenes substituted with aniline tetramer. The  $\pi$  systems of the oligoaniline side group and the 2,5-thienylene main chain are not in conjugation in this case because they are separated by a nonconjugated spacer. The developed hybrid copolymer

should distinguish itself by the versatility of its processing methods, as processing techniques used for polyalkylthiophenes and those typically applied for polyaniline can be exploited. Moreover, because of the presence of two isolated redox systems in a conductive matrix, which are, in addition, of chromophore nature, one can expect interesting pH-dependent voltammetric and spectroelectrochemical behaviors of the polymer.

In this paper, we briefly describe the preparation of poly(octylthiophene) with pendant tetraaniline groups, discuss its supramolecular organization, and characterize its voltammetric and spectroelectrochemical (UV–vis, Raman) properties. We also study its chemical doping with  $FeCl_3$  using  $^{57}Fe$  Mössbauer spectroscopy.

## Experimental Section

**Reagents and Chemicals.** 3-Octylthiophene was prepared from 3-bromothiophene by Kumada coupling as described elsewhere.<sup>19</sup> Ethyl 3-thiopheneacetate (98% Aldrich), was vacuum distilled (66 °C, 2 mmHg) prior to its use. Aniline tetramer in the oxidation state of emeraldine was prepared as described in ref 17. THF (pure; POCh, Gliwice, Poland) was fractionally distilled from potassium and benzophenone after a color change to navy blue and then stored over dried 4 Å molecular sieves.  $CH_3NO_2$  (97%, ROTH) and  $CCl_4$  (pure for analysis; POCh, Gliwice, Poland) were dried over  $CaCl_2$  and then distilled.

$FeCl_3$  (anhydrous, 98%; Fluka), 4-dimethylaminopyridine (abbreviated as DMAP, 99%; Aldrich),  $N,N'$ -dicyclohexylcarbodiimide (abbreviated as DCC, 99%; Fluka), HCl (35–38%, pure for analysis; POCh, Gliwice, Poland), NaOH (pure for analysis; POCh, Gliwice, Poland), and  $CH_3OH$  (pure for analysis; POCh, Gliwice, Poland) were used as received.

**Characterization Techniques.** Both the precursor copolymer, i.e., poly(3-octyl-2,5-thienylene-*co*-3-methylene-ethylcarboxylate-2,5-thienylene), and the final copolymer containing aniline tetramer side groups were identified by  $^1H$  NMR and FTIR spectroscopies. In the latter case, elemental analysis was also performed.

NMR spectra were recorded on a Varian Mercury 400 MHz spectrometer with chloroform-*d* ( $CDCl_3$ ) solvent. FTIR spectra were recorded on an FTIR Bio-RAD FTS 165 spectrometer (wavenumber range, 400–4000  $cm^{-1}$ ; resolution, 4  $cm^{-1}$ ) either on free-standing films cast from chloroform or using the KBr pellet technique. UV–vis–NIR spectra of thin solid films or solutions in chloroform were recorded on a UV–vis Perkin-Elmer Lambda 2 spectrometer.

Molecular weight determinations of the synthesized polymers were made using size-exclusion chromatography (SEC) on a Shimadzu LC-10 AD chromatograph equipped with a Nucleogel M-10 column, using refractometric detection by an RID-6A refractometer. THF was used as the eluent. The column temperature and the flow rate were fixed to 35 °C and 1  $mL \cdot min^{-1}$ , respectively. The column was calibrated using polystyrene standards provided by Polymer Standards Service.

Wide-angle X-ray diffraction (WAXD) studies of the neutral polymers were carried out in  $\theta/2\theta$  reflection geometry using Cu  $K\alpha$  radiation (1.542 Å). The scan step was 0.04° (in  $2\theta$ ) with a counting time of 17 s/step. The diffractometer was equipped with a linear 800-channel multidetector, giving a 16° window in  $2\theta$ .

(13) Łapkowski, M.; Berrada, K.; Quillard, S.; Louarn, G.; Lefrant, S.; Pron, A. *Macromolecules* **1995**, *28*, 1233.

(14) Daoust, G.; Leclerc, M. *Macromolecules* **1991**, *24*, 455.

(15) Cao, Y.; Smith, P.; Heeger, A. J. *Synth. Met.* **1992**, *48*, 91.

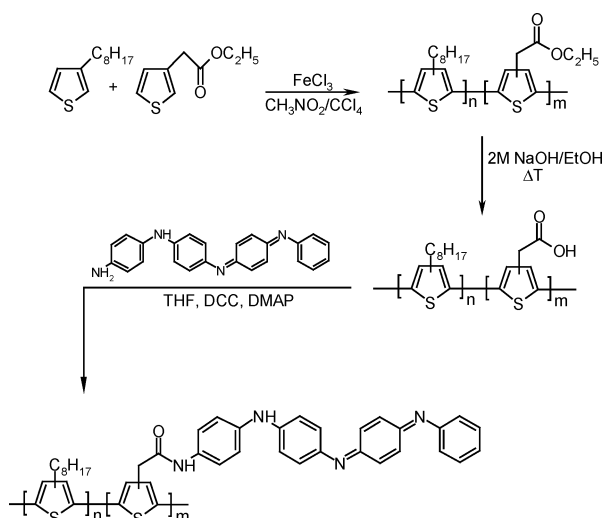
(16) Chen, R.; Benicewicz, B. C. *Macromolecules* **2003**, *36*, 6333.

(17) Dufour, B.; Rannou, P.; Travers, J. P.; Pron, A.; Zagorska, M.; Korc, G.; Kulszewicz-Bajer, I.; Quillard, S.; Lefrant, S. *Macromolecules* **2002**, *35*, 6112.

(18) Buga, K.; Kepczynska, K.; Kulszewicz-Bajer, I.; Zagórska, M.; Demadrille, R.; Pron, A.; Quillard, S.; Lefrant, S. *Macromolecules* **2004**, *37*, 769.

(19) Tamao, K.; Kodama, S.; Nakajima, S.; Kumala, M.; Minato, A.; Suzuki, A. *Tetrahedron* **1982**, *38*, 3347.

Scheme 1



Free-standing films for the diffraction studies were obtained by casting from  $\text{CHCl}_3$  solution.

Mössbauer spectra of  $\text{FeCl}_3$ -doped poly(octylthiophene) containing aniline tetramer side groups were measured at 77 K. In a drybox, the samples were loaded into a tight polyamide container prior to the experiment and immediately transferred to the cryostat of the spectrometer. The typical thickness of the absorber was  $2 \text{ mg} \cdot \text{cm}^{-2}$  of natural iron.  $\text{Co(Rh)}$  was used as a Mössbauer source. A  $\text{Na}_2(\text{CN})_5 \cdot 2\text{H}_2\text{O}$  absorber operating at room temperature was used for the velocity calibration. The spectra were recorded in a constant-acceleration mode and analyzed with a least-squares procedure.

For cyclic voltammetry investigations, a thin layer of the polymer was deposited on a platinum disk electrode by casting from chloroform solution. The experiments were carried out in a one-compartment electrochemical cell with a Pt counterelectrode and an  $\text{Ag}/(0.1 \text{ M AgNO}_3 \text{ in acetonitrile})$  double-junction reference electrode using an AUTOLAB potentiostat (Ecochemie, The Netherlands). The electrolyte consisted of a mixture of 0.1 M tetrabutylammonium tetrafluoroborate (TBATFB) and 0.1 M diphenyl phosphate (DPP) in acetonitrile, the latter serving as a source of protons facilitating the redox processes associated with the grafted aniline tetramer.<sup>13</sup> The same electrolyte, reference electrode, and counter electrode were used in the case of UV-vis-NIR and Raman spectroelectrochemical studies. A thin polymer film was deposited on an ITO transparent working electrode in the former case and on a platinum plate electrode in the latter. The UV-vis-NIR spectra were measured on a Lambda 2 Perkin-Elmer spectrometer, whereas the Raman spectra were obtained using an FT Raman Bruker RFS 100 spectrometer with the near-IR excitation line (1064 nm).

**Synthesis of Polymer with Grafted Tetraaniline Groups.** The sequence of reactions used for the preparation of the functionalized poly(octylthiophene) with pendant aniline tetramer is depicted in Scheme 1.

First, 3-octylthiophene and ethyl-3-thiopheneacetate are copolymerized to give poly(3-octyl-2,5-thienylene-co-3-methylene-ethylcarboxylate-2,5-thienylene) (**P1**). Subsequent hydrolysis of the ester groups in **P1** yields **P2**, which, after grafting of aniline tetramer via an amidation reaction, is converted into **P3**, i.e., a polymer in which the main chain consists of 2,5-thienylene groups to which alkyl and aniline tetramer side groups are attached.

The synthesis of precursor polymer **P1** was carried out in a  $\text{CCl}_4/\text{CH}_3\text{NO}_2$  mixed solvent with  $\text{FeCl}_3$  as the oxidizing/polymerizing agent using a procedure similar to that described in ref 20. The polymerization details can be found elsewhere.<sup>18</sup> Size-exclusion chromatography (SEC) measurements gave the number-average

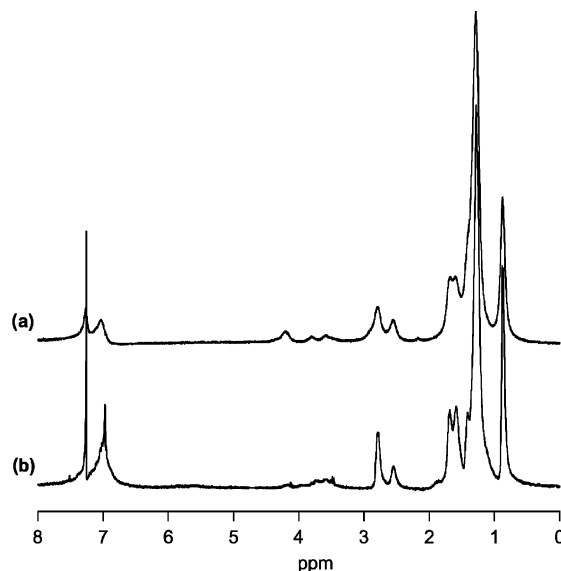


**Figure 1.**  $^1\text{H}$  NMR spectra of (a) poly(3-octyl-2,5-thienylene-co-3-methylene-ethylcarboxylate-2,5-thienylene), the precursor polymer (**P1**); (b) the hybrid polymer obtained after the postpolymerization grafting of aniline tetramer (**P3**) in  $\text{CDCl}_3$ .

molecular mass,  $M_n = 13\,800 \text{ g/mol}$ , with a dispersity coefficient equal to 5.24. It should be noted that the  $M_n$  value of polythiophene derivatives, obtained using polystyrene standards, is significantly overestimated and, for molecular weights higher than  $10\,000 \text{ g/mol}$ , the overestimation coefficient exceeds 2.<sup>21</sup> Such a rather high polydispersity coefficient is typical of polythiophenes obtained via oxidative polymerization using  $\text{FeCl}_3$ .<sup>22</sup>

The precursor polymer was then hydrolyzed to give the corresponding polyacid, **P2**. The hydrolysis procedure used was a modification of the method described in ref 23. In this reaction, 0.1 g of the precursor polymer was dissolved in 5 mL of  $\text{CHCl}_3$ , and then 10 mL of 2 M NaOH solution in EtOH was added dropwise. The mixture was then heated to the boiling temperature, and the reaction was carried out under reflux for 24 h. The product, in the form of a red suspension, was separated by filtration on a Büchner funnel, stirred in 2 M HCl/methanol solution (5:1) for a few hours, and finally vacuum-dried.

The reaction of aniline tetramer grafting was carried out under a dry nitrogen flow using a procedure frequently applied to esterification or amidation reactions.<sup>24</sup> In this procedure, 162 mg of the hydrolyzed polymer was dissolved in 20 mL of dry THF. Then, a solution of 112 mg (0.3 mmol) of aniline tetramer in 10 mL of dry THF, 63 mg (0.3 mmol) of DCC, and 4 mg of DMAP were consecutively added. The reaction was stopped after 18 h. In the next step, THF was removed on a rotary evaporator, and the remaining polymer was repeatedly washed with methanol until the filtrate was colorless. Finally, the obtained polymer powder was dried in a vacuum line to constant mass.

In Figure 1, the  $^1\text{H}$  NMR spectra recorded for the precursor polymer **P1** and for the final product containing tetraaniline pendant groups **P3** are compared. The composition of the precursor polymer can be estimated from the ratio of the integrated signals at 0.87

- (20) Costa Bizzarri, P. C.; Andreani, F.; Della Casa, C.; Lanzi, M.; Salatielli, E. *Synth. Met.* **1995**, *75*, 141.
- (21) Liu, J.; Loewe, R. S.; McCullough, R. D. *Macromolecules* **1999**, *32*, 5777.
- (22) Demadrille, R.; Rannou, P.; Bleuse, J.; Oddou, J. L.; Pron, A.; Zagorska, M. *Macromolecules* **2003**, *36*, 7045.
- (23) Kim, B. S.; Chen, L.; Gong, J.; Osada, Y. *Macromolecules* **1999**, *32*, 3964.
- (24) Neises, B.; Steglich, W. *Angew. Chem., Int. Ed. Engl.* **1978**, *17*, 522.



and 4.19 ppm, which correspond to the methyl group of the octyl substituent and the methylene group adjacent to oxygen in the ester substituent, respectively. The normalization of these signals per one proton gives the molar ratio of the octyl groups to the ester groups as 1:0.23. The hydrolysis and tetraaniline grafting sequence leads to a complete disappearance of the signal attributed to the methylene group in the ester substituent, as expected (compare Figure 1a and b). The combustion analysis confirms the NMR data; however, a good fit of the analytical data can be obtained only if the hydration of each nitrogen with one water molecule is assumed [calcd for  $-(C_{12}H_{18}S)_{1.0}-(C_{30}H_{22}SN_4 \cdot 4H_2O)_{0.23}-$  %C = 70.36, %H = 7.72, %N = 3.99; found %C = 69.26, %H = 7.72, %N = 3.90]. This is a reasonable assumption taking into account the hydrophilic character of polyaniline and its oligomers.

The precursor polymer **P1** gives a clear IR spectrum in which bands characteristic of the two coexisting subunits, i.e., 3-octyl-2,5-thienylene and 3-methylene-ethylcarboxylate-2,5-thienylene, are present. The hydrolysis of **P1** followed by tetraaniline grafting results in the appearance of new bands characteristic of oligoanilines. In particular, the broad band at ca.  $3350\text{ cm}^{-1}$  can be ascribed to N–H stretchings in the grafted tetramer. This band is accompanied by a band of lower intensity at  $3054\text{ cm}^{-1}$ , typical of C–H stretches in the phenylene ring. Other important bands corroborating the grafting of the tetramer can be found at 1595, 1509, and  $1496\text{ cm}^{-1}$ .<sup>25</sup> The formation of the amide bond, occurring upon tetramer grafting, is manifested by a shift of the band corresponding to the C=O stretching deformation from  $1737\text{ cm}^{-1}$  in the precursor polymer to the wavenumbers typical for amides (ca.  $1660\text{ cm}^{-1}$ ). The IR spectra of **P1** and **P3** are included in the Supporting Information, whereas the attribution of all characteristic bands can be found elsewhere.<sup>18,26</sup>

**Doping of the Hybrid Polymer with FeCl<sub>3</sub>.** Chemical doping of **P3** was carried out in a vacuum-tight apparatus using a 0.05 M solution of FeCl<sub>3</sub> in dried acetonitrile. The excess of the doping agent was removed by repeated washing with pure acetonitrile. Finally, the doped polymer was dried to constant mass in a vacuum line.

## Results and Discussion

The electrochemical and spectroelectrochemical properties of thin solid films of the precursor (**P1**) and the postfunctionalized (**P3**) polymers depend not only on the chemical composition of their individual chains but also on the type of the supramolecular organization that they form. For this reason, we undertook WAXD studies of both polymers. Their diffractograms are compared in Figure 2a. The diffraction pattern of **P1** is remarkably similar to those reported for poly-(3-alkylthiophene)s obtained by oxidative polymerization.<sup>27–29</sup> In these compounds, a strong and narrow reflection is observed at low Bragg angles whose position is dependent on the length of the substituent. For this reason, this reflection is attributed to the distance between the stacks of polymer chains separated by alkyl side groups, which—depending on

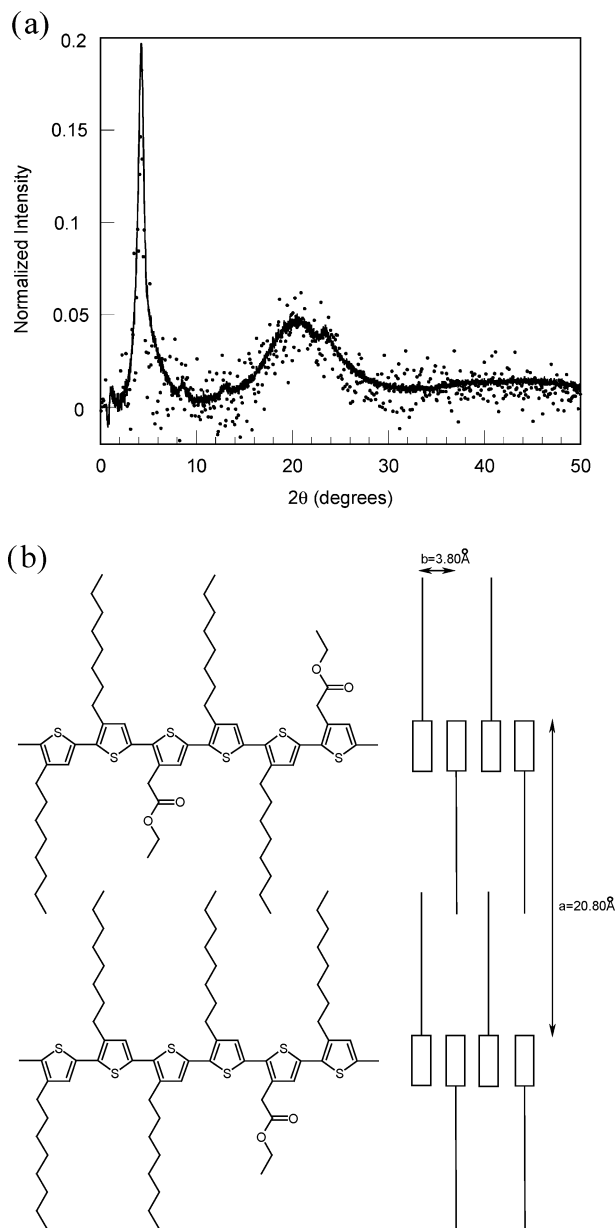


**Figure 2.** (a) X-ray diffraction patterns (in reflection Bragg–Brentano geometry, Cu K $\alpha$ ) obtained for free-standing films of **P1** (solid line) and **P3** (experimental points). (b) Idealized model of the supramolecular organization of the precursor polymer, **P1**. One ester substituent is depicted per four alkyl substituents, consistent with the NMR data and elemental analysis. The distribution of the substituents, however, is random.

their length—are more or less interdigitated. This ordered supramolecular organization, in the direction perpendicular to the chain stacking direction, is surprising considering that the oxidative polymerization is not regiospecific and, as a result, the distribution of the alkyl substituents is not uniform because of the presence of a significant number of head-to-head and tail-to-tail couplings in addition to the predominant head-to-tail couplings. Evidently, this irregularity has a stronger negative impact on the structural order along the chains than on the organization in the lateral direction.

According to this perspective, the precursor polymer, which is a random copolymer of 3-octylthiophene and ethyl 3-thiopheneacetate with dominating alkylthiophene units, should behave similarly. Thus, taking into account the Bragg reflections present in the diffractogram of **P1**, for the ordered

(25) Zhang, W. J.; Feng, J.; MacDiarmid, A. G.; Epstein, A. J. *Synth. Met.* **1997**, *84*, 119.

(26) Garreau, S.; Leclerc, M.; Erlen, N.; Louarn, G. *Macromolecules* **2003**, *36*, 692.

(27) Samuelsen, E. J.; Mardalen, J. In *Handbook of Organic Conductive Molecules and Polymers*; Nalwa, H. S., Ed. John Wiley & Sons: New York, 1997; Vol. 3, p 87.

(28) Winokur, M. J.; Walmsley, P.; Moulton, J.; Smith, P.; Heeger, A. J. *Macromolecules* **1991**, *24*, 3812.

(29) Luzny, W.; Trznadel, M.; Pron, A. *Synth. Met.* **1996**, *81*, 71.

parts of this polymer, we are tempted to propose a structural model similar to that reported for orthorhombic poly(3-alkylthiophene)s (see Figure 2b). However, the deconvolution of the diffraction peaks, presented in the Supporting Information, clearly indicates that the observed "crystalline" reflections are superimposed on broad features originating from less ordered parts. In particular, the dominant (100) reflection ( $2\theta = 4.25^\circ$ ,  $d = 20.8 \text{ \AA}$ ) and its second-order (200) counterpart ( $2\theta = 8.50^\circ$ ,  $d = 10.4 \text{ \AA}$ ) are superimposed on a broad amorphous halo peaked at  $4.70^\circ$  ( $d = 20.55 \text{ \AA}$ ). Note that the distance corresponding to the (100) reflection implies very little interdigitation of the lateral alkyl chains because twice the length of the octyl group ( $22.2 \text{ \AA}$ ) only slightly exceeds the interchain distance ( $20.8 \text{ \AA}$ ). The two other crystalline reflections at  $2\theta = 23.60^\circ$  ( $d = 3.80 \text{ \AA}$ ) and  $2\theta = 13.00^\circ$  ( $d = 6.66 \text{ \AA}$ ) are, in turn, superimposed on a broad peak originating from the alkyl interchain correlation distance ( $2\theta = 20.60^\circ$ ,  $d = 4.30 \text{ \AA}$ ). The former crystalline peak corresponds to the interchain distance in the chain stacking direction and should be indexed as (001). The attribution of the latter is more difficult. In the literature, it is indexed either as the (300) third-order reflection<sup>27</sup> or as the sum of (120), (020), and (300) reflections.<sup>29</sup> Taking into account that its  $d$  value is significantly smaller than  $d(100)/3$  and its intensity is comparable to the intensity of the second-order reflection (200), we would rather index this reflection as (020).

The next problem to be addressed is the effect of the exchange of the ester groups in the precursor polymer, **P1**, for the tetraaniline ones on the supramolecular organization in the resulting, postfunctionalized polymer, **P3**. For clarity, the diffraction pattern of **P3**, which shows a poor signal-to-noise ratio, is presented in the form of experimental points, whereas the pattern of **P1** is indicated by the solid line (see Figure 2a). Despite a big difference in their quality, a striking similarity of the two diffractograms can be noticed. This applies to the reflection at  $2\theta = 4.25^\circ$  (100), the reflection at  $2\theta = 23.60^\circ$  (001), and the alkyl interchain correlation distance at  $2\theta = 20.60^\circ$ . This finding is rather surprising given that the length of the grafted aniline tetramer in its rectal (all trans) form ( $24 \text{ \AA}$ ) should exceed the interchain distance in the  $a$  direction ( $20.8 \text{ \AA}$ , see Figure 2b). It is therefore postulated that the grafted aniline tetramer side chains are forced to be tilted in or out of the  $ab$  plane. This is, of course, possible considering the variety of possible conformations in this substituent and should not affect the reflections corresponding to the (100) and (001) planes.

Poly(octylthiophene) containing pendant oligoaniline groups contains two types electrochemically active chromophores and, for this reason, is very well suited for combined voltammetric–spectroelectrochemical investigations. As has already been stated, all voltammetric and spectroelectrochemical studies were carried out in TBATFB/acetonitrile electrolyte to which a source of protons (diphenyl phosphate) was added with the goal of facilitating the redox processes that, in the case of grafted tetramer, involve not only the charge transfer but also the proton transfer. A representative cyclic voltammogram of **P3** is shown in Figure 3. Two overlapping anodic peaks can be distinguished with maxima at ca. 0.25

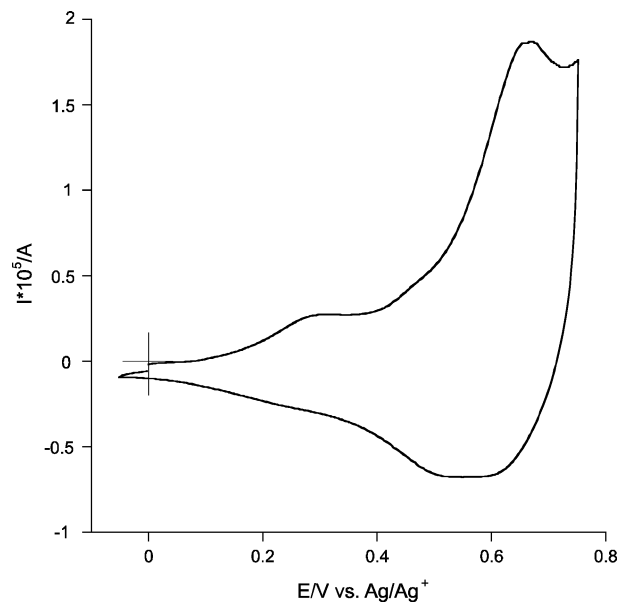


**Figure 3.** Cyclic voltammogram of the hybrid polymer obtained in 0.1 M TBATFB/0.1 M DPP/acetonitrile electrolyte. Scan rate, 50 mV/s; reference, Ag/0.1 M Ag<sup>+</sup>.

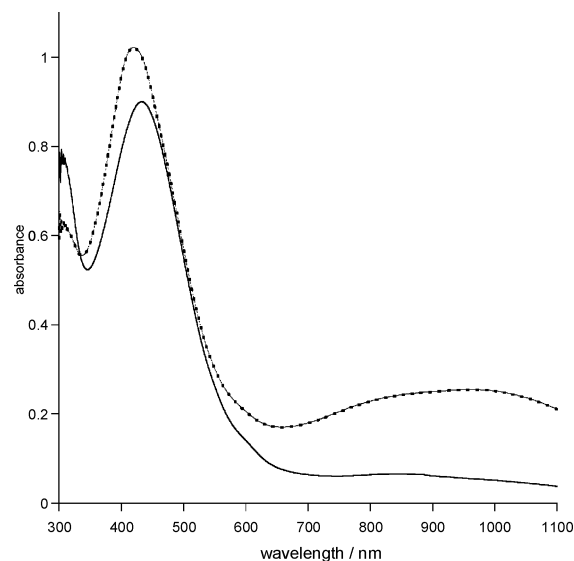
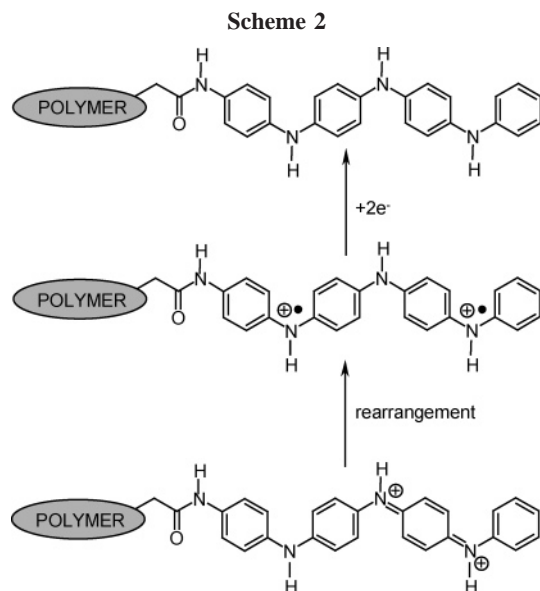


**Figure 4.** UV–vis–NIR spectra (up to 1100 nm) of the hybrid polymer deposited on an ITO electrode and in contact with the electrolyte (0.1 M TBATFB/0.1 M DPP/acetonitrile) at the open-circuit potential ( $E_{oc} = +0.22 \text{ V}$ ,  $E$  vs Ag/0.1 M Ag<sup>+</sup> (dotted line) and after its reduction at  $E = -0.20 \text{ V}$ ,  $E$  vs Ag/0.1 M Ag<sup>+</sup> (solid line).

and 0.67 V, together with their cathodic counterparts. One is tempted to ascribe the first oxidation peak of lower intensity to the oxidative doping of the tetraaniline side group and the dominant peak to the doping of the polythiophene main chain. In reality, the first spectroscopic signs of the polythiophene backbone oxidation appear for potentials as low as  $E = +0.30 \text{ V}$ , i.e., just above the maximum of the first oxidation peak. This is, of course, caused by the facts that the two anodic peaks strongly overlap and that the second oxidation process current makes some contribution to the first anodic peak. We carried out a detailed spectroscopic and spectroelectrochemical investigations to elucidate this problem.

In Figure 4, the open-circuit voltage spectrum (dotted line) of the postfunctionalized polymer deposited on an ITO



electrode is presented. It is clear that, in the electrolyte used (0.1 M TBATFB/0.1 M DPP/acetonitrile), the grafted aniline tetramer side groups undergo protonation. The broad absorption band, covering the spectral range from ca. 650 to 1100 nm (the limit of the spectrometer used), is characteristic of the protonated aniline oligomer in the semi-oxidized (emeraldine) oxidation state. The imposition of the potential  $E = -0.2$  V leads to the reduction of the grafted tetramer to the totally reduced state of leucoemeraldine. As a result, all spectroscopic features characteristic of the semi-oxidized state disappear, and the recorded spectrum contains two bands at 300 and 433 nm characteristic of the reduced, neutral tetraaniline side chains and the neutral polythiophene main chain, respectively. Note that, for the former, only the lower-energy part of the band is shown. The reduction of the semi-oxidized aniline tetramer is facilitated by its protonation in the electrolytic medium given that the electrochemical process in this case involves only a simple charge transfer, as shown in Scheme 2.

**P3** contains two types of electrochemically active chromophores that, in addition, exhibit different redox and acid–base chemistries. Thus, the spectroelectrochemical response of this polymer is complex. The UV–vis–NIR spectra (up to 1100 nm) of **P3**, recorded in the oxidation mode, i.e., for increasing electrode potentials, are shown in Figure 5. For clarity, the spectra obtained in three different potential zones are presented and discussed separately:  $-0.20$  V  $< E < +0.25$  V,  $+0.25$  V  $< E < +0.60$  V, and  $+0.60$  V  $< E < +0.80$  V.

In the first potential zone, up to  $E = +0.05$  V, both electroactive components of the postfunctionalized polymer, i.e., the conjugated polythiophene main chain and the grafted aniline tetramer, are in the undoped reduced state. At  $E = +0.1$  V, the first spectroscopic signs of the electrochemical oxidation appear, i.e., a decrease in the intensity of the band at 300 nm [the  $\pi$ – $\pi^*$  transition band in the reduced (neutral) tetraaniline side chain] with concomitant growth of a broad absorption tail extending from ca. 650 nm to the near-infrared region. These changes, indicative of gradual transformation of the neutral, reduced aniline tetramer into its semi-oxidized protonated form, become more pronounced with increasing

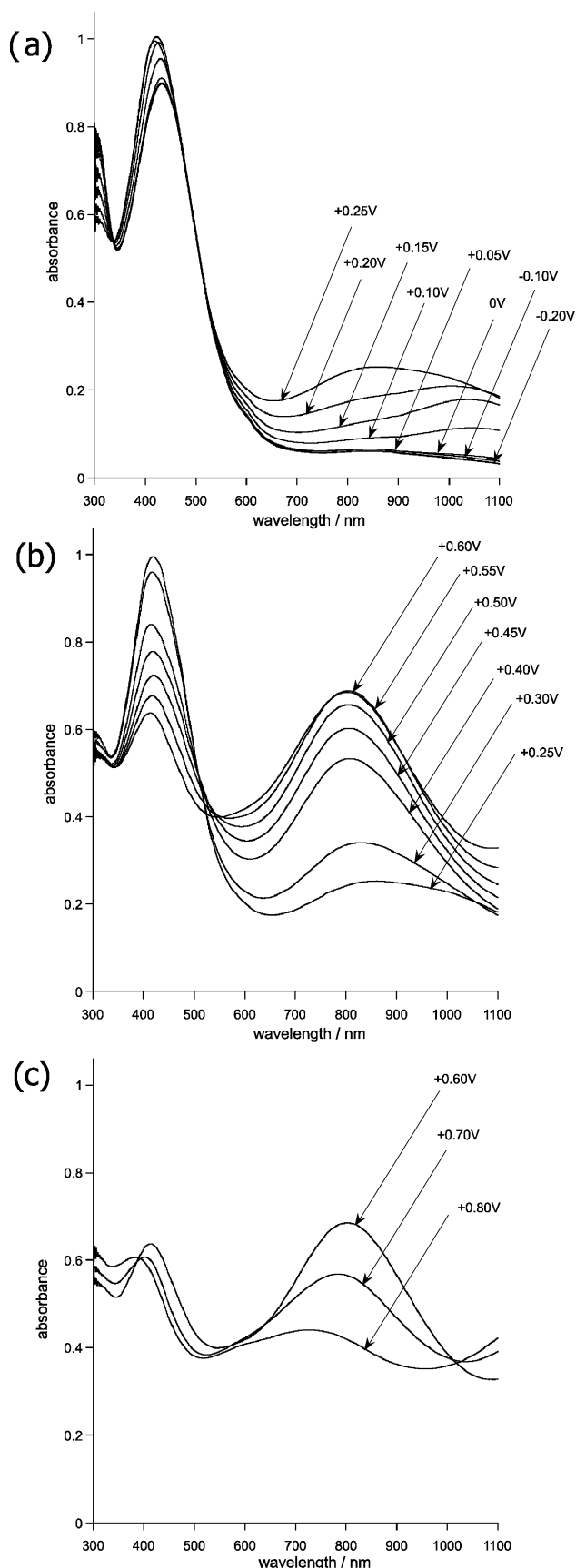


**Figure 5.** UV–vis–NIR spectra (up to 1100 nm) of the hybrid polymer recorded for increasing electrode potential (0.1 M TBATFB/0.1 M DPP/acetonitrile electrolyte; Ag/0.1 M Ag<sup>+</sup> reference. Potential range: (a)  $-0.20$  V  $< E < +0.25$  V, (b)  $+0.25$  V  $< E < +0.60$  V, (c)  $+0.60$  V  $< E < +0.80$  V.

electrode potential. It should be noted that, at  $E = +0.25$  V, the spectrum of the polymer film becomes very similar to

that recorded for the open-circuit potential (compare Figures 4 and 5a). Because the polymer main chain is in its neutral reduced state and the aniline tetramer is in its oxidized protonated state at  $E_{oc}$ , it can be concluded that, in the potential range  $-0.2 \text{ V} < E < +0.25 \text{ V}$ , only the grafted oligoaniline side groups undergo electrochemical oxidation, the main chain remaining intact. This conclusion is further corroborated by an apparent increase of the intensity of the  $\pi$ - $\pi^*$  transition band of the neutral polythiophene main chain at ca. 430 nm. Any oxidative doping of the main chain should give rise to an opposite effect, i.e., a decrease in the intensity of the  $\pi$ - $\pi^*$  transition band. This apparent increase of the peak intensity is caused by the fact that the absorption band, essentially unchanged in this potential range, is superimposed on the increasingly intense absorption background caused by the oxidation of the side-group aniline tetramer to its semi-oxidized protonated form.

The oxidative doping of the polythiophene main chain starts at  $E > +0.25 \text{ V}$  and is spectroscopically manifested by a gradual bleaching of the band originating from the  $\pi$ - $\pi^*$  transition in the conjugated main chain. At the same time, the doping induced bipolaron bands grow. The first of them is superimposed on the broad absorption feature associated with the protonated aniline tetramer side groups, the second being beyond the limits of the spectrometer used, so that only its onset can be seen for  $E = +0.6 \text{ V}$  (see Figure 5b).

For  $E > +0.6 \text{ V}$  (see Figure 5c), the first bipolaronic band starts to decrease in intensity and undergoes a hypsochromic shift. For  $E = +0.8 \text{ V}$ , this band is transformed into a broad absorption extended toward the near-infrared region. In the case of polythiophene and its derivative, such behavior is indicative of the transition from the bipolaronic state into the quasimetallic state.<sup>30</sup>

At the end of this part, it should be noted that a very good correlation between the shape of the polymer cyclic voltammogram and the UV-vis-NIR spectroelectrochemical response can be found if one compares Figures 3 and 5. First, we notice that the spectroscopically determined onset of the aniline tetramer side-group oxidation coincides with the onset of the first anodic peak. Second, the doping of the polythiophene main chain, as probed by gradual bleaching of the  $\pi$ - $\pi^*$  transition band at ca. 430 nm, starts at the potential of the maximum of the first oxidation peak. Finally, just above the potential of the second oxidation peak maximum, spectroscopic features of the transition from the bipolaronic state to the quasimetallic one appear.

Oxidative and acid-base dopings of polyconjugated systems give rise to symmetry and chain conformation changes and also influence the force constants of selected bonds as a result of charge or proton transfer. All of these phenomena are reflected in the vibrational spectra, and for this reason, Raman spectroscopy is a very convenient tool for the investigation of both chemical and electrochemical doping of conjugated polymers. One must, however, be aware of the fact that conjugated polymers contain various

types of chromophores that, depending on the energy of the excitation line, can induce resonant enhancement of selected Raman bands. In the case of both poly(alkylthiophene)s<sup>31</sup> and polyaniline,<sup>13</sup> it is known that both the positions and the intensities of the principal Raman bands depend on the energy of the excitation line. For this reason, it is difficult to extract quantitative data from Raman spectroelectrochemical investigations. However, valuable qualitative information can be obtained provided that the Raman spectroelectrochemical response is analyzed in correlation with UV-vis-NIR spectra. In particular, for the infrared excitation line ( $\lambda_{exc} = 1064 \text{ nm}$ ) used in this research, Raman resonant enhancement is expected for the vibrations of those structural segments that give rise to significant absorbance values in the 1000–1100 nm spectral region. This means that  $\lambda_{exc} = 1064 \text{ nm}$  is out of resonance with as-prepared **P3** in which the oligoaniline side groups are in the semi-oxidized base state and the polythiophene main chain is in its neutral reduced state, as no significant absorbance value is measured in its UV-vis-NIR spectrum in the vicinity of the energy of the excitation line. Extended FT Raman measurements of a solid film of **P3** result in a spectrum with a rather poor signal-to-noise ratio (not shown here) whose principal bands at 1600, 1480, 1380, and 1173  $\text{cm}^{-1}$  are very similar to those reported for polyaniline in the form of emeraldine base recorded using the same excitation line.<sup>32</sup> The lines at 1480 and 1380  $\text{cm}^{-1}$  might include the contributions from the two most intense Raman bands originating from the neutral polythiophene chain, which, unfortunately, coincide with the bands of oligoaniline.<sup>31</sup> Under the conditions of the spectroelectrochemical experiment, i.e., for the film of **P3** in contact with nonacidified 0.1 M TBATFB/acetonitrile electrolyte, it was not possible to obtain a measurable spectrum (see Figure 6). Acidification of the electrolyte results in a significant improvement of the resonance conditions (see the value of the absorbance of the protonated form of **P3** at 1064 nm, at the open-circuit potential, presented in Figure 4). As a consequence, the protonated form of aniline tetramer gives a much better Raman spectrum (Figure 6). The spectrum of the grafted tetramer in the semi-oxidized protonated state, recorded at the open-circuit potential, is almost identical to that obtained for electrochemically prepared polyaniline in its semi-oxidized state, protonated with the same acid and studied using the same excitation line ( $\lambda_{exc} = 1064 \text{ nm}$ ).<sup>13</sup> The bands originating from the polythiophene main chain are practically “invisible”, with the exception of the strongest band, which is present as a small peak at 1495  $\text{cm}^{-1}$ . All of these spectral features clearly indicate that only the tetramer part of the hybrid polymer is in resonance. The reduction of the polymer at  $E = -0.2 \text{ V}$  again leads to a worsening of the resonance conditions because it results in a strong decrease of the absorbance at 1064 nm (see Figure 4). In the Raman spectrum of the reduced polymer, only residual peaks of small intensity, originating from incompletely reduced segments, can be distinguished (Figure 6). This is

(30) Chung, T. C.; Kaufman, J. H.; Heeger, A. J.; Wudl, F. *Phys. Rev. B* **1984**, *30*, 702.

(31) Louarn, G.; Trznadel, M.; Buisson, J. P.; Laska, J.; Pron, A.; Lapkowski, M.; Lefrant, S. *J. Phys. Chem.* **1996**, *100*, 12532.

(32) Laska, J.; Girault, R.; Quillard, S.; Louarn, G.; Pron, A.; Lefrant, S. *Synth. Met.* **1995**, *75*, 69.



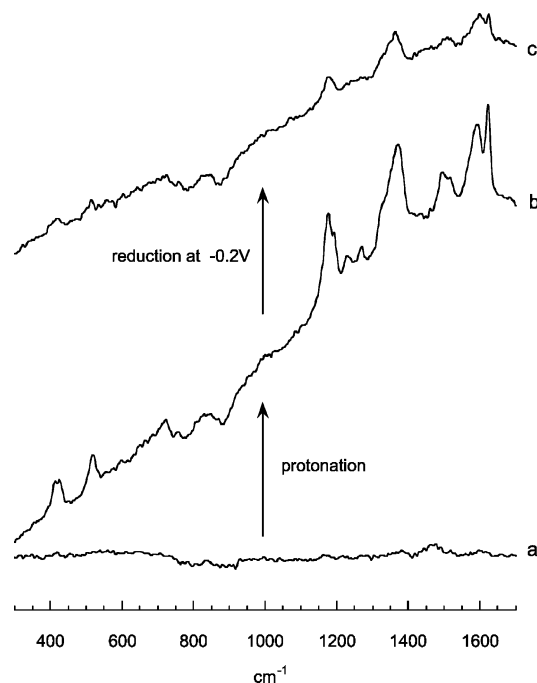


**Figure 6.** Raman spectra of the hybrid polymer deposited on a Pt electrode,  $\lambda_{\text{exc}}=1064$  nm, recorded (a) after the grafting reaction in contact with the 0.1 M TBATFB/acetonitrile electrolyte, (b) after acidification of the electrolyte with 0.1 M DPP (open-circuit potential  $E_{\text{oc}} = +0.22$  V), (c) after reduction at  $E = -0.20$  V in the acidified electrolyte (potential vs Ag/0.1 M  $\text{Ag}^+$  reference).

an obvious manifestation of the resonance effect because minute amounts of incompletely reduced parts are detected whereas the dominating fully reduced side oligoaniline groups and the neutral main polythiophene chain remain “invisible” for the Raman spectroscopy.

The evolution of the Raman spectra of the postfunctionalized polymer, during its oxidation from the fully reduced forms of both electroactive components (aniline oligomer and polythiophene backbone) to their fully oxidized states, is depicted in Figure 7. Up to  $E = +0.10$  V, no evolution of the spectrum can be detected, which indicates that the resonant conditions do not improve. At this potential, an abrupt increase in the intensity of the four principal bands ( $1623$ ,  $1597$ ,  $1373$ , and  $1178$   $\text{cm}^{-1}$ ), characteristic of the protonated semi-oxidized oligoaniline side groups, occurs.<sup>13</sup> This is understandable because the oxidation of the tetramer from the leucoemeraldine state to the protonated emeraldine state gives rise to a significant increase in the absorbance value in this part of the spectrum, which matches the energy of the excitation line used ( $1064$  nm; see Figure 5). Consistent with the UV-vis-NIR finding, the polythiophene main chain remains intact; with no resonance enhancement, its vibrations are undetectable. In the potential range  $+0.1$  V  $< E < +0.55$  V, the bands originating from the protonated semi-oxidized oligoaniline side groups dominate the spectrum, obviously because of the improved resonance conditions. The first indication of the oxidative doping of the polythiophene main chain appears at  $E = 0.6$  V, i.e., at the potential that is  $0.3$  V higher than in the case of the UV-vis-NIR studies. This apparent discrepancy can again be explained taking into account the resonance phenomena. Evidently, the growth of the bipolaronic bands, which accompanies the oxidative doping of the polythiophene main

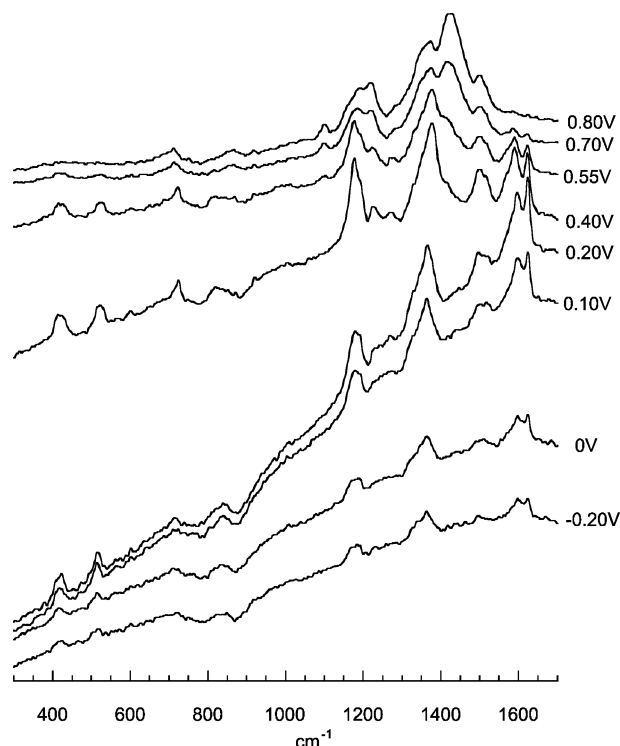


**Figure 7.** Raman spectra of the hybrid polymer deposited on a Pt electrode, recorded for increasing electrode potentials  $\lambda_{\text{exc}}=1064$  nm; potential vs Ag/0.1 M  $\text{Ag}^+$  reference; 0.1 M TBATFB/0.1 M DPP/acetonitrile electrolyte.

chain, does not contribute to the absorbance at  $\lambda = 1064$  nm whose value remains determined by the component originating from the semi-oxidized side oligoaniline groups. Thus, the oxidized segments of the main chain cannot be detected in this potential range. The situation changes for higher potentials, at which the bipolaronic state is gradually being transformed into the quasimetallic one. For  $E > +0.7$  V, the peaks originating from the tetramer side groups become undetectable, and the bands characteristic of the oxidatively doped polythiophene main chain dominate the spectrum. In the quasimetallic state, the contribution of the polythiophene absorption tail to the absorbance at  $\lambda = 1064$  nm becomes dominant, causing resonance enhancement of the polythiophene bands at the expense of the oligoaniline ones. We only note here that the principal bands at  $1499$  and  $1428$   $\text{cm}^{-1}$  correspond to  $\text{C}_\alpha\text{--C}_\beta$  antisymmetric and symmetric stretches in the doped polythiophene chain, the band at  $1375$   $\text{cm}^{-1}$  originates from  $\text{C}_\beta\text{--C}_\beta$  stretches, and the band at  $1221$   $\text{cm}^{-1}$  corresponds to  $\text{C}_\alpha\text{--C}_\alpha'$  inter-ring stretching deformations. A detailed discussion of the Raman spectroscopic features of the oxidatively doped polythiophene chain can be found in ref 31.

Finally, a very good correlation between the onset and different steps of the postfunctionalized polymer oxidative doping, as detected by cyclic voltammetry and UV-vis-NIR and Raman spectroelectrochemistries, should be underlined. In the latter case, the resonance phenomena must be considered, however.<sup>33–36</sup>

One of the specific features of the postfunctionalized polymer, **P3**, is the possibility of its global doping with, for example,  $\text{FeCl}_3$ . Because **P3** consists of a neutral polythiophene chain and aniline tetramer side groups in the



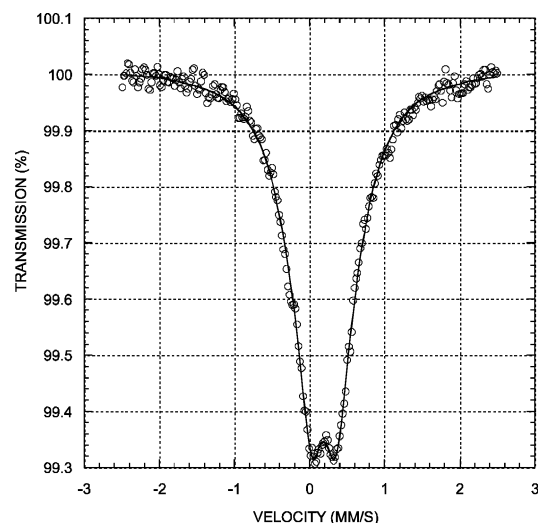


**Figure 8.**  $^{57}\text{Fe}$  Mössbauer spectrum of the hybrid polymer doped chemically with  $\text{FeCl}_3$ , measured at 77 K.

oxidation state of emeraldine, two types of doping are possible: oxidation of the main chain to a polycation with simultaneous formation of  $\text{FeCl}_4^-$  as the dopant species<sup>33,34</sup> and formation of an acid–base complex in the Lewis sense between  $\text{FeCl}_3$  and the basic centers of the oligoaniline substituents.<sup>35</sup> The former gives rise to one Mössbauer doublet, whereas in the latter, two doublets originating from the complexation on amine and imine sites usually coexist. The Mössbauer spectrum of  $(\text{C}_{12}\text{H}_{18}\text{S})_{1.0}-(\text{C}_{30}\text{H}_{22}\text{SN}_4)_{0.24}$  doped with  $\text{FeCl}_3$  is shown in Figure 8. The content of the dopant (15 wt %) was determined gravimetrically from the increase of the weight of the sample after the doping reaction. In the globally (main chain and side group) doped polymer, one should expect three doublets corresponding to one type of doping sites in the main chain and two types (imine and amine) of doping sites in the oligoaniline substituents. However, the Mössbauer spectrum obtained cannot be deconvoluted into three doublets. A reasonably good fit is obtained only for two doublets of similar isomer shifts (ISs) and a very different quadrupole splitting (QS) values. The calculated Mössbauer parameters are collected in Table 1. We are tempted to interpret the inner doublet as originating from  $\text{FeCl}_4^-$  anions compensating the charge of the doped main chain because the Mössbauer parameters are very similar to those reported for doped polythiophene.<sup>33,34</sup>

The outer doublet should therefore originate from the complexation of  $\text{FeCl}_3$  on basic sites of the oligoaniline substituent. Combining Mössbauer spectroscopy, indicating

**Table 1.** Mössbauer Parameters of  $\text{FeCl}_3$ -Doped Hybrid Polymer (**P3**) Measured at 77 K<sup>a</sup>

	IS (mm/s) <sup>b</sup>	QS (mm/s) <sup>c</sup>	$\Gamma$ (mm/s) <sup>d</sup>
external doublet 50%	0.29(1) <sup>e</sup>	0.68(6)	0.79(8)
internal doublet 50%	0.30(1)	0.32(1)	0.39(2)

<sup>a</sup> Sample composition:  $-(\text{C}_{12}\text{H}_{18}\text{S}^{+0.14})_{1.0}-(\text{C}_{30}\text{H}_{22}\text{SN}_4)_{0.24}(\text{FeCl}_4^-)_{0.14}-(\text{FeCl}_3)_{0.14}$ . <sup>b</sup> IS is the isomer shift relative to  $\alpha$  Fe at room temperature.

<sup>c</sup> Quadrupole splitting ( $\text{QS}$ ) =  $1/2 e^2 q Q$ . <sup>d</sup>  $\Gamma$  is the full width at half-maximum given for a Lorentzian line. <sup>e</sup> Errors are given in parentheses, in units corresponding to the last digit of the quoted values.

a ca.1:1 ratio of both types of dopants, with gravimetry, we obtain the following formula for the doped polymer:  $-(\text{C}_{12}\text{H}_{18}\text{S}^{+0.14})_{1.0}-(\text{C}_{30}\text{H}_{22}\text{SN}_4)_{0.24}(\text{FeCl}_4^-)_{0.14}(\text{FeCl}_3)_{0.14}$ .

In ref 36, the effect of the doping level on the Mössbauer parameters of the dopant complexed on imine and amine sites is discussed for  $\text{FeCl}_3$ -doped polyaniline. In particular, it is shown that the QS value increases with decreasing doping level for all complexing sites. The IS and QS values calculated for the outer doublet in **P3** doped with  $\text{FeCl}_3$  are in the range expected for  $\text{FeCl}_3$  complexed on amine sites, but exceed the value reported for  $\text{PANI}(\text{FeCl}_3)_{0.5}$ —the lowest doping level studied by these authors. However, the doping level normalized per nitrogen atom, in the case of  $\text{FeCl}_3$  complexed on the oligoaniline part of **P3**, is even smaller (0.15), which might lead to increased QS values. The oligomer nature of the complexing side group as well as its grafting to the polythiophene chain, which modify the closest coordination of the Mössbauer nuclei, might also contribute to this difference. One should also note that the width ( $\Gamma$ ) of the lines corresponding to the external doublet is large (see Table 1), which reflects the distribution of the IS values caused by the fact that, at low doping levels, the complexing sites might not be completely equivalent.

## Conclusions

To summarize, by postpolymerization functionalization, we have prepared a solution-processible hybrid polymer consisting of a polythiophene main chain and aniline tetramer side groups. The proposed method is more versatile than previously used copolymerization methods because it enables the preparation of polymers with much higher grafting levels. Moreover, as shown by spectroscopic studies, the polymer can be selectively doped in its side chains or globally in the main chain and in the side chains.

**Acknowledgment.** Some of the authors (K.B., A.M., R.P., M.Z.) acknowledge partial financial support by Warsaw University of Technology.

**Supporting Information Available:** Additional figures showing FTIR spectra, solution UV–vis–NIR spectra, and deconvolution of X-ray diffraction peaks. This material is available free of charge via the Internet at <http://pubs.acs.org>.

CM050794M

- (33) Kitao, S.; Matsuyama, T.; Seto, M.; Maeda, Y.; Masubuchi, S.; Kazama, S. *Synth. Met.* **1995**, *69*, 371.
- (34) Kulszewicz-Bajer, I.; Pron, A.; Suwalski, J.; Kucharski, Z.; Lefrant, S. *Synth. Met.* **1989**, *28*, C225.
- (35) Genoud, F.; Kulszewicz-Bajer, I.; Bedel, A.; Oddou, J. L.; Jeandey, C.; Pron, A. *Chem. Mater.* **2000**, *12*, 744.
- (36) Kulszewicz-Bajer, I.; Suwalski, J. *Synth. Met.* **2001**, *119*, 343.